



Tree rings and rainfall in the equatorial Amazon

Daniela Granato-Souza¹ · David W. Stahle² · Ana Carolina Barbosa¹ · Song Feng² · Max C. A. Torbenson² · Gabriel de Assis Pereira¹ · Jochen Schöngart³ · Joao Paulo Barbosa⁴ · Daniel Griffin⁵

Received: 25 October 2017 / Accepted: 25 April 2018 / Published online: 8 May 2018
© Springer-Verlag GmbH Germany, part of Springer Nature 2018

Abstract

The Amazon basin is a global center of hydroclimatic variability and biodiversity, but there are only eight instrumental rainfall stations with continuous records longer than 80 years in the entire basin, an area nearly the size of the coterminous US. The first long moisture-sensitive tree-ring chronology has been developed in the eastern equatorial Amazon of Brazil based on dendrochronological analysis of *Cedrela* cross sections cut during sustainable logging operations near the Rio Paru. The Rio Paru chronology dates from 1786 to 2016 and is significantly correlated with instrumental precipitation observations from 1939 to 2016. The strength and spatial scale of the precipitation signal vary during the instrumental period, but the Rio Paru chronology has been used to develop a preliminary reconstruction of February to November rainfall totals from 1786 to 2016. The reconstruction is related to SSTs in the Atlantic and especially the tropical Pacific, similar to the stronger pattern of association computed for the instrumental rainfall data from the eastern Amazon. The tree-ring data estimate extended drought and wet episodes in the mid- to late-nineteenth century, providing a valuable, long-term perspective on the moisture changes expected to emerge over the Amazon in the coming century due to deforestation and anthropogenic climate change.

Keywords Equatorial Amazon · *Cedrela* · Tree rings · Precipitation · Sea surface temperature · ENSO

1 Introduction

The Amazon basin is one of the largest centers of deep atmospheric convection on earth and it plays a major role in the general circulation of the atmosphere and the global energy balance (Crutzen 1987; Wang and Fu 2007; Hilker et al. 2014). The hydroclimatology of the Amazon basin may be changing because drought and wetness extremes have both increased in frequency over portions of the basin since 1960 (Lewis et al. 2011; Gloor et al. 2013; Marengo and

Espinoza 2016). This apparent amplification of the hydrologic cycle over the Amazon has been hypothesized to arise from both natural and anthropogenic factors, including interactions between deforestation and climate over the Amazon (Gentry and Lopez-Parodi 1980; Costa et al. 2003; Calde et al. 2004; Chagnon and Bras 2005; Khanna et al. 2017), anthropogenic alterations to global climate (IPCC 2013; Nobre et al. 2016), increased water vapor transport from the warmer tropical North Atlantic (Gloor et al. 2013), decadal sea surface temperature (SST) changes in the Pacific (Gloor et al. 2015), or it may simply be due to the large natural variability of Amazonian hydroclimate. Just how unprecedented these recent moisture extremes might be in the context of natural climate variability is impossible to determine from the short, sparse, and frequently interrupted instrumental precipitation and streamflow records for Amazonia.

The longest continuous precipitation measurements in the entire 7.5×10^6 km² drainage basin of the Amazon River begin in 1892 at Rio Branco in the western Amazon and in 1901 at Manaus, Brazil (based on the stations included in the CRU TS4.00 gridded precipitation data set; Harris et al. 2014). The longest hydrological observation in the Amazon is the stage height record of the Rio Negro at Manaus

✉ David W. Stahle
dstahle@uark.edu

¹ Department of Forest Sciences, Federal University of Lavras, Lavras, MG 37200-000, Brazil

² Department of Geosciences, University of Arkansas, Fayetteville, AR 72701, USA

³ Instituto Nacional de Pesquisas da Amazonia (INPA), Manaus 69060-001, Brazil

⁴ Department of Biology, Federal University of Lavras, Lavras, MG 37200-000, Brazil

⁵ Department of Geography, University of Minnesota, Minneapolis, MN 55455, USA

that began continuous measurements in 1903 (Richey et al. 1989). However, only eight instrumental rainfall records longer than 80 years with less than 10% missing values are available for the entire basin, an area nearly the size of the coterminous US. Very high-resolution precipitation proxies will be necessary to extend the instrumental record in the Amazon in order to evaluate the apparent amplification of moisture extremes in the context of natural climatic variability during the late Holocene.

Moisture sensitive tree-ring chronologies provide excellent seasonal and annual proxies of precipitation in the middle latitudes (e.g., Fritts 1966; Villalba et al. 1998; Griffin et al. 2013), but have been very difficult to develop in the moist tropics due to the scarcity of native tree species with clear annual growth rings that can be exactly dated to their calendar year of formation. However, annual tree-ring chronologies have recently been developed in the western Amazon basin (Bräuning et al. 2009; Lopez and Villalba 2011; Paredes-Villanueva et al. 2016), and a well dated and replicated tree-ring reconstruction of wet season rainfall totals was reported by López et al. (2017) for the headwaters of the Madeira River in the southern Amazon basin. These chronologies were based on the dendrochronological crossdating of ring width time series, but Baker et al. (2015) demonstrate that oxygen isotope measurements on the growth rings can enhance crossdating of selected tropical species in the western Amazon. In this paper we describe the development of the first exactly dated and well-replicated ring-width chronology in the eastern equatorial Amazon basin of Brazil. We document the precipitation signal in this tree-ring chronology, use the chronology to estimate precipitation variability over the eastern Amazon for the past 231 years, and examine the large-scale climate dynamics involved in the inter-annual variability of instrumental and reconstructed precipitation over this sector of Amazonia.

2 Background to the tree ring collections

An estimated 16,000 tree species may be native to the lowland forests of the Amazon (ter Steege et al. 2013), but only 6727 have been described taxonomically (Cardoso et al. 2017). A small fraction of the known tree species (227) are actually found widely across the basin and represent $\pm 50\%$ of the 390 billion individual trees estimated to be present in the lowland Amazon (ter Steege et al. 2013). This includes *Cedrela odorata*, which has been found in 96 of the study plots tabulated by ter Steege et al. (2016). A few of these “hyperdominant” species form annual growth rings (Schöngart et al. 2017) and may be suitable for the development of a geographic network of climate sensitive tree-ring chronologies as has been possible in the mid-to high-latitudes

of the Northern and Southern Hemisphere (e.g., Meko et al. 1993; Cook et al. 1999; Villalba et al. 2012).

We have collaborated with logging companies and Norte Energia, the large energy conglomerate responsible for the construction of the Belo Monte hydroelectric project on the Rio Xingu to obtain cross-sections for tree ring analysis (Fig. 1). These companies have legal authority for sustainable forestry or full deforestation in construction zones. With the cooperation of the owners of these firms, their managers, and employees we were able to cut full and partial cross-sections from recently felled trees. As part of this collaboration, all tree-ring specimens collected under the auspices of Norte Energia, CEMAL, and other firms have been cataloged and permanently stored in the archives of the Tree Ring Laboratories at the Federal University of Lavras and the National Institute for Amazonian Research (INPA) where they are available for further scientific research.

Chainsaw operators employed by our collaborating firms cut all of these research cross sections. To facilitate these collections we developed a guide in Portuguese to explain the procedures for cutting specimens for tree-ring analysis. This guide is illustrated in Fig. 2 and highlights where the samples should be cut on the felled trees. Some specimens were obtained in the forest where the trees were actually felled, but many were collected at log yards (*pátios*) where recently cut logs were stored prior to shipment (Fig. 3). Only general provenience (± 10 km) is known for the specimens obtained from the *pátios*.

Our target species were *Bertholletia excelsa* (Lecythidaceae), *Cedrela fissilis* and *Cedrela odorata* (Meliaceae), and *Macrolobium acaciifolium* (Fabaceae), all of which have wide distributions in the Amazon. *Bertholletia excelsa*, the Brazil nut tree, is a protected and socioeconomically important tree species that is not harvested by our collaborating logging companies. However, hundreds of *Bertholletia* had to be cut during the construction of the Belo Monte project. We collected cross-sections from 212 *B. excelsa* trees from the Rio Xingu region, which is believed to be the largest collection of *Bertholletia* cross sections currently available. *Macrolobium acaciifolium* is a dominant floodplain species with low economic value and thus far we have collected cores and cross-sections from over 200 *Macrolobium* trees the eastern Amazon on the Rio Tapajós and Rio Xingu.

Cedrela fissilis and *C. odorata* are both native in the eastern Amazon and in some cases these species have clear and unambiguous annual rings useful for tree-ring dating elsewhere in the basin (Dünisch et al. 2002; Brienen et al. 2012). Cross-sections from 47 legally harvested *Cedrela* sp. were obtained from an old growth State-owned forest near the Rio Paru (Fig. 1) that has been recently opened to sustainable timber production and 45 were collected from the Belo Monte project on the Rio Xingu. It is not possible to identify the species of *Cedrela* from the wood anatomy alone, but we

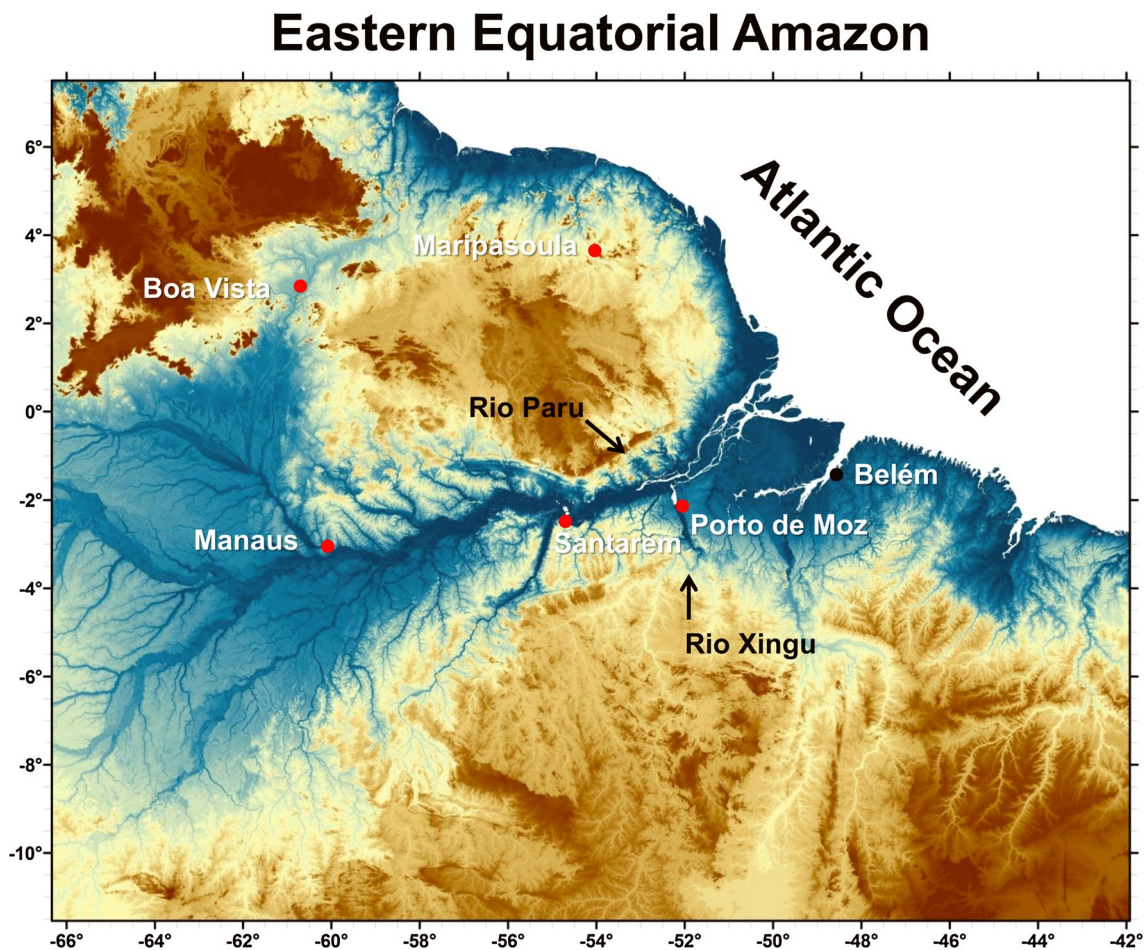


Fig. 1 The tree-ring collection sites on the Rio Paru and Rio Xingu are located on this terrain map of the eastern Amazon River basin. The *Cedrela* specimens were collected just west of the Rio Paru and

near the southern escarpment of the Guiana Highlands at 200 m elevation. The locations of the weather recording stations included in these analyses are also indicated (red symbols)

believe that *C. odorata* dominates our collections from the Rio Paru because it is the only species of *Cedrela* cited in the forest inventory of CEMAL, the operator of the forest concession on the Rio Paru. The analyses reported below are all based on *Cedrela* from the Rio Paru in the eastern equatorial Amazon.

3 Data and methods

3.1 Sample preparation and tree-ring analysis

Cross-sections were dried and highly polished to reveal the minute cellular anatomy of the annual rings. Most tropical hardwoods have complex xylem anatomy, but previous research has proven that annual rings can be formed in *Cedrela* (Brienen and Zuidema 2005; Paredes-Villanueva et al. 2016). In some *Cedrela* stands, the symmetry of the concentric growth rings can be distorted by competition

among trees for light, insect attack (Dünisch et al. 2002), and senescence (Lopez and Villalba 2016). But the well-formed concentric growth rings in the *Cedrela* sections from the Rio Paru site are exceptionally clear (Fig. 4) and the time series patterns were easily matched among trees.

The annual growth rings of the Rio Paru *Cedrela* were crossdated using skeleton plots and visual dating under the microscope (Douglass 1941; Stokes and Smiley 1996). The dated ring widths were measured to a precision of 0.001 mm and the derived time series were submitted to dating and measurement quality control with the computer program COFECHA (Holmes 1983). The correctly dated series were carefully detrended and standardized by fitting cubic smoothing splines to remove non-synchronous and likely non-climatic multi-decadal to centennial growth trends using the program ARSTAN (Cook 1985; Cook and Krusic 2005). The derived tree-ring indices were computed by dividing the measured ring-width value for each year by the value of the fitted curve for the same year (ratios). The final robust mean

ESTUDO DOS ANÉIS DE ÁRVORES: RECONSTRUINDO O CLIMA

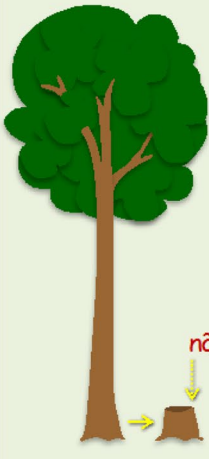
GUIA DE AMOSTRAGEM

1 O QUE CORTAR?

Amostras do tronco de árvores de **CEDRO** (*Cedrela odorata* e *Cedrela fissilis*).

Para cada sítio (área com um raio de 10 km), são necessárias em torno de 100 amostras.

Se na área a espécie for abundante, dar preferência para as maiores e mais velhas, mas também algumas menores. *proporção de aproximadamente 80% grandes e 20% médias)

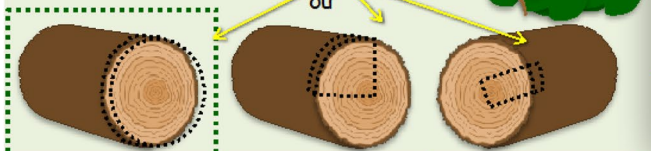


2 COMO CORTAR?

Corte uma seção transversal no final da primeira tora * não na base/toco

Tentar cortar duas faces paralelas:

- ✓ Espessura das amostras: 5-6 cm
- ✓ Largura do corte radial: 20-25 cm
- ✓ Cortes de pizza e radial: mais de uma amostra, preferencialmente.



“CORTE DISCO”
(disco completo)

“CORTE PIZZA”
(1/4 - 1/8 disco)

“CORTE RADIAL”
corte retangular

O CORTE IDEAL
Primeira e melhor opção

*** INCLUIR A MEDULA E CASCA**
Tentar incluir o anel central, alborno e último anel formado abaixo da casca

Identificar a amostra:

- Código de identificação da empresa
- Data de abate da árvore
- Se a árvore já está morta, indicar “morta”
- Código da espécie (CEOD, CEFI ou CESP*)

* CEOD: *C. odorata* CEFI: *C. fissilis* CESP: *Cedrela sp.*

3 ONDE CORTAR A AMOSTRA?



1. Selecione região de forma a evitar cicatrizes, canais de resinas, crescimento anômalo (nem sempre possível)

2. Se a medula não estiver no centro, selecione região de maior crescimento

3. Árvores sólidas ou com pouco oco podem ser amostradas

4. Árvores muito ocas não devem ser amostradas.

4 COMO GUARDAR?

Armazenar as amostras dispostas verticalmente em local seco e ventilado (para evitar empenamento).

Deixar espaço para circulação do ar entre as amostras.



◀**Fig. 2** This is the Portuguese language guide to the collection of thin cross-sections from tropical trees felled during construction projects or under legal and sustainable logging concessions

index standard chronology was obtained by averaging all ring width index series on a year-by-year basis (Cook 1985; Cook and Krusic 2005). These detrending and standardization procedures were designed to maximize the high- to medium-frequency (e.g., interannual to decadal) coherence between the tree-ring time series because the lower frequency variance in these relatively short records does not strongly synchronize among trees and may arise primarily from age trend and stand dynamics in these closed forest environments. A series of statistics were computed with the ARSTAN program to describe the internal consistency of the individual ring width series and of the derived standard chronology [e.g., mean sensitivity, mean correlation among all series (RBAR; Cook and Pederson 2011), and the expressed population signal (EPS; Wigley et al. 1984)].

Note that the “Schulman Shift” was not applied to the dating of the Rio Paru chronology. This means that tree growth occurring in the 2016 calendar year was assigned to 2016 and not 2015 as it would have been using the “shift” which has been the Southern Hemisphere standard since Schulman’s pioneering tree-ring research in the 1950s (Schulman 1956). Based on limited observations and informant information, most annual radial growth in *Cedrela* trees at Rio Paru appears to take place during the wet season (February–July; see also Wagner et al. 2014), so it seems reasonable to assign annual dating to the rings during the year in which they are largely formed in these near equatorial forests.

3.2 Growth-climate analyses

The Rio Paru *Cedrela* chronology was correlated spatially with monthly precipitation totals in the Climatic Research Unit (CRU) TS4.00 0.5° gridded data set from 1900 to 2015 (Harris et al. 2014) and in the Global Precipitation Climatology Centre (GPCC) V7 0.5° data set from 1901–present (Becker et al. 2013; Schneider et al. 2017), maximum and minimum temperatures (HadCRUTS4.01; Harris et al. 2014), and the Palmer Drought Severity Index (CRUscPDSI3.25; van der Schrier et al. 2013) to identify the strongest monthly or seasonal climate signals. An experimental reconstruction of February–November precipitation totals was developed using the point-by-point regression (PPR) method of Cook et al. (1999, 2010) to calibrate the standardized ring width chronology from the Rio Paru with a four-station average of instrumental precipitation data from the eastern Amazon extracted from the CRU TS4.00 data set (i.e., Porto de Moz, Santarem, Manaus, and Boa Vista). The tree-ring chronology was calibrated from 1939 to 1970 with normalized February–November total precipitation

using a bivariate regression model. The derived reconstruction was then validated against just a 20-year period 1971–1990 because the data available for Porto de Moz and Santarem in the CRU TS4.00 compilation end in 1990. To estimate the uncertainty of the tree-ring estimates each year, semi-parametric 90% prediction intervals described by Cook et al. (2013) and based on both standard least squares theory (Seber and Lee 2003; Olive 2007) and the maximum entropy bootstrap method (Vinod 2006) used to randomly rearrange the predictor and predictand were computed for each year of the reconstruction. Additional climate analyses were performed using station precipitation data for Maripasoula, French Guiana (CRU TS4.00, Harris et al. 2014), the COBE Sea Surface Temperature data set (Ishii et al. 2005), and NCEP/NCAR reanalysis data (Kalnay et al. 1996). These analyses were computed using the unfiltered instrumental and reconstructed time series, and with filtered versions emphasizing interannual to subdecadal and decadal to multidecadal components of the rainfall series isolated with a nine-point binomial filter.

4 Results

We analyzed the annual growth rings on cross sections from 47 trees cut near the Rio Paru with dendrochronology. A total of 56 dated and measured radii from 27 separate trees were used to construct a fully replicated chronology that dates from 1786 to 2016 (RBAR 0.246; Fig. 5). Many of the trees that were not included in the chronology are in fact datable with dendrochronology, but they were either young trees with short time series or suffered other irregularities in growth and were excluded from these analyses. A second chronology was also developed from a subset of the 10 oldest and most highly cross-correlated trees (27 total radii; RBAR 0.319; Fig. 5). Both dated tree ring data sets are highly correlated ($r=0.91$ from 1786 to 2016, $r=0.90$ from 1901 to 2016), but the most internally coherent chronology from the ten best trees has a stronger correlation with monthly precipitation values and is used in all subsequent climate comparisons and reconstructions.

Exploratory analyses using both the CRU and GPCC gridded precipitation data sets indicated that the Rio Paru *Cedrela* ring-width chronology is positively correlated with monthly instrumental precipitation observations available from the eastern Amazon during most months of the calendar year for the period 1939–2015 when the observations are most complete. However, the strength and spatial scale of the correlations seem to have shifted over this interval (Fig. 6a–d). The period with the strongest and most widespread precipitation signal is 1939–1970 when the chronology was correlated with February–November rainfall over the eastern equatorial Amazon and into Venezuela and



Fig. 3 A typical collection of tropical hardwood logs felled during construction of the Belo Monte hydroelectric project on the Rio Xingu. All felled trees were cataloged, identified to species and prepared for sale. Hundreds of hardwood cross-sections were obtained from these logs with the assistance of Norte Energia, and are preserved in the Tree-Ring Laboratory at the Federal University of Lavras, Brazil



Fig. 4 This polished cross-section illustrates the clear annual growth rings on a *Cedrela* sp. cross-section cut during a legal operation near the Rio Paru (this portion of the specimen dates from 1785 (pith) to 1856, decades noted with white marks). The annual growth rings of this species are readily distinguished by semi-ring porosity and marginal parenchyma. The micro ring at 1833 is locally absent and difficult to see in this image

Columbia (Fig. 6a). From 1971 to 2015 the area of significant positive precipitation correlation is restricted to the extreme eastern Amazon and Guiana Highlands (Fig. 6b). The near-annual February–November precipitation totals appear to be most highly correlated with the tree-ring chronology (Fig. 6a, b), but the chronology is also significantly correlated with March–May rainfall totals during the heart of the wet season in the vicinity of the Rio Paru during both subperiods of the instrumental era (Fig. 6c, d). The Rio Paru chronology was also correlated with gridded temperature and PDSI for the Amazon basin, but the results were much weaker than for precipitation, likely due in part to the very limited number of long temperature records from the region.

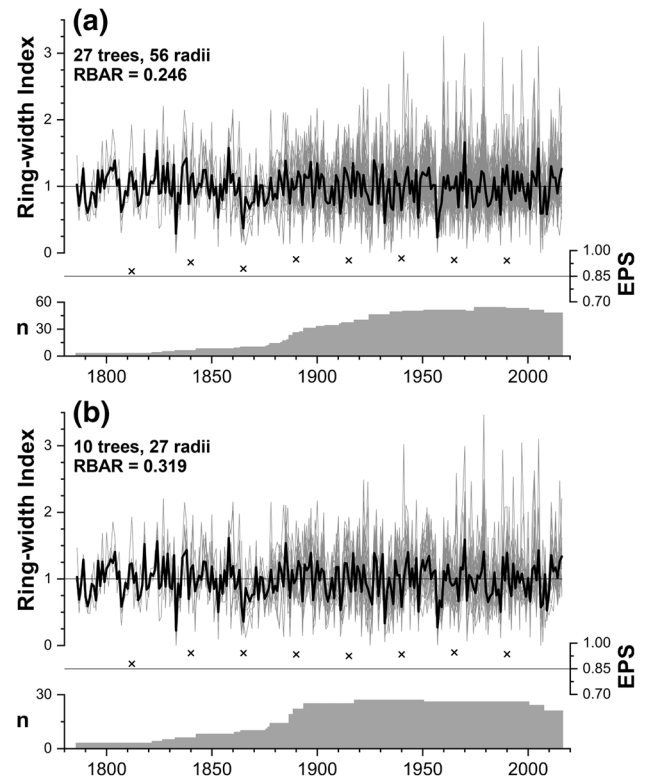


Fig. 5 **a** The 56 tree-ring dated and measured radii from 27 *Cedrela* trees obtained from the Rio Paru are plotted as detrended, standardized and autoregressively modeled white noise residuals (gray time series). The mean index residual chronology is also plotted (black), both for the fully replicated set of 56 radii and **b** a subset of the 27 radii from 10 trees that are longest and most strongly correlated among all component radii (i.e., RBAR 0.246 and 0.319, respectively). Both data sets pass the 0.85 EPS threshold test for all 50-year subperiods (overlapping 25 years). The changing sample size of dated radii is plotted below each panel

The Rio Paru site is located less than one degree south of the equator where it may be affected by the two leading modes of rainfall variability in northeastern South America. Empirical orthogonal function (eof) analysis of GPCP wet season (MAM) precipitation totals from 1939 to 2013 identifies a dipole in rainfall variability north and south of the equator that represents 23.8% of the precipitation variance (eof1, Fig. 7a; see also Torralba et al. 2015). The second mode of variance (eof2) highlights variability largely confined to the eastern and central equatorial Amazon River sector, which is the mode that would tend to be represented by the four-station precipitation average that straddles the equator (i.e., Porto de Moz, Santarem, Manaus, and Boa Vista; Figs. 1, 7b). The changes in the spatial pattern of correlation between the tree-ring data and rainfall (Fig. 6) might be due in part to temporal variations in the influence of these modes of rainfall variability (e.g., Torralba et al. 2015).

In spite of the changes in strength and spatial pattern of precipitation correlation (Fig. 6), rainfall variability

Rio Paru Chronology Spatial Correlation with Rainfall

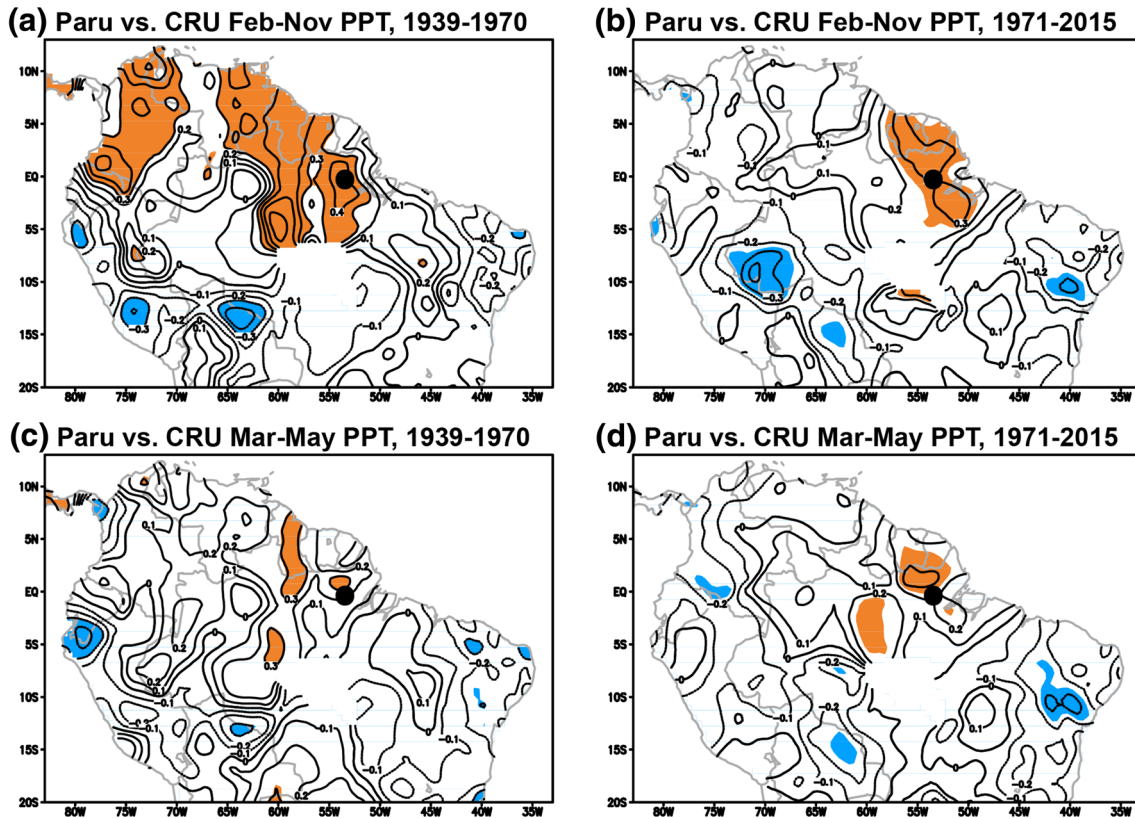


Fig. 6 The spatial pattern of correlation computed between the standard chronology from the Rio Paru and CRU TS 4.00 0.5° gridded February–November total precipitation is illustrated for 1939–1970 (a), and 1971–1990 (b). The Rio Paru chronology (black dot) is also correlated with CRU 3-month precipitation totals during the heart

of the wet season (March–May) for both subperiods, 1939–1970 (c) and 1971–2015 (d; significant positive correlations shaded orange, negative in blue, $p < 0.10$). A data void area is located near 10°S and 55°W

appears to be the primary climate signal reflected by the coherent ring width variability in the Rio Paru chronology. This is supported by the significant positive correlations in Fig. 6a–d, by the correlation with select wet season rainfall totals [e.g., MAM at Maripasoula, French Guiana ($r = 0.37$; $p < 0.01$, 1961–2016)], and by the significant positive correlation between the Rio Paru chronology and annual maximum river levels for the Rio Negro at Manaus during the full common interval of 1903–2015 ($r = 0.25$; $p < 0.01$). It is also possible to calibrate and validate the Rio Paru chronology with February–November precipitation totals observed in the eastern equatorial Amazon during the 1939–1990 period.

To define the optimal season and region for this preliminary tree-ring reconstruction of precipitation, a regional average of the four longest monthly precipitation stations in the eastern Amazon was computed using Porto de Moz, Santarem, Manaus, and Boa Vista, which are largely complete from 1939 to 1990 (a few missing monthly values were

replaced in the station observations with monthly means). The Rio Paru tree-ring chronology is positively correlated with precipitation during most months of the year concurrent with growth (Fig. 8). The highest correlations were calculated for February and March, which is the beginning of the wet season (generally February to July) in this region of the eastern Amazon (e.g., Torralba et al. 2015). The driest months of the year generally include August and September, but the tree-ring chronology remains positively correlated with monthly totals for the 10-month extending from February through November (Fig. 8).

The correlation of the tree-ring chronology with 10-month total precipitation (February–November) for the four-station average from 1939 to 1990 is strong enough to develop an experimental tree-ring reconstruction of precipitation for the equatorial Amazon (note that the regional precipitation average was computed from the normalized station totals). The chronology explains 37% of the instrumental

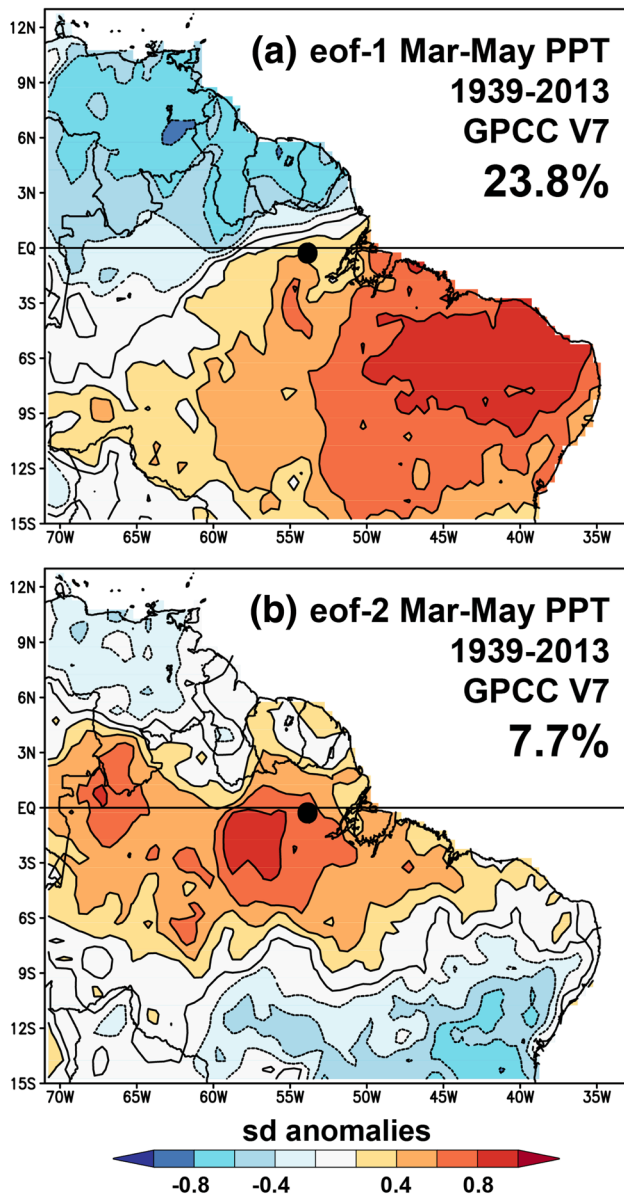


Fig. 7 The spatial anomaly patterns associated with the two leading modes of precipitation variability in northeastern South America are mapped [eof1 (a) and eof2 (b)] based on GPCP March–May precipitation totals, 1939–2013 (similar results were observed for 10-month February–November precipitation totals and using the CRU TS4.00 precipitation data). The percent variance represented by each mode is listed and the location of the Rio Paru tree-ring chronology is noted on both maps (black dot). The eof1s were computed using the KNMI Climate Explorer (<https://climexp.knmi.nl>)

precipitation variance during the 1939–1970 calibration period (adjusted $R^2 = 0.375$; no lead or lag versions of the tree-ring chronology were selected as predictors; Fig. 9), and the cross validation reduction of error computed for the same interval is $CVRE = 0.356$. The reconstruction compares reasonably well with the independent instrumental precipitation data during the short 1971–1990 validation interval. For the

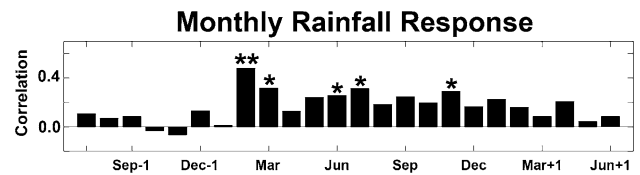


Fig. 8 The monthly values for the four-station regional precipitation average were correlated with the Rio Paru standard chronology from 1939 to 1990 to identify the monthly precipitation totals most important to the radial growth of *Cedrela* from the Rio Paru for a 24-month period including 6 months prior to (–1) and following (+1) the year concurrent with growth. Significant correlations are noted with asterisks (* $p < 0.05$, ** $p < 0.01$; the highest single monthly correlation is February, $r = 0.49$)

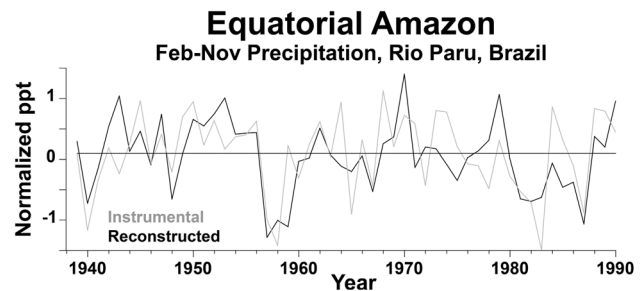
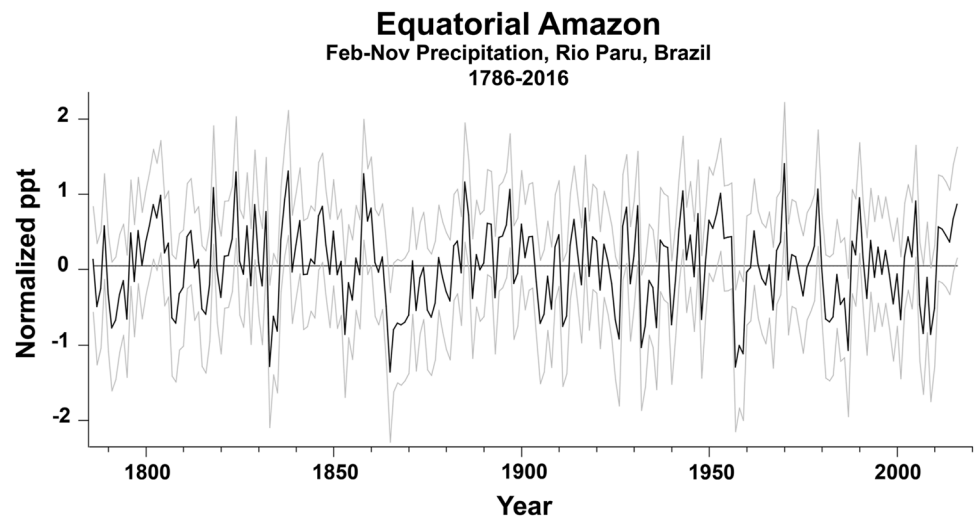


Fig. 9 The instrumental (gray) and reconstructed (black) February–November precipitation totals for the eastern equatorial Amazon are plotted together from 1939 to 1990. The tree-ring chronology was calibrated with instrumental precipitation from 1939 to 1970 ($RSQ_{adj} = 0.375$) and validated from 1971 to 1990 (Pearson $R^2 = 0.275$)

period 1971–1990, the Pearson R^2 is 0.275, the RE is 0.288, and the coefficient of efficiency (CE) is 0.273 (Cook et al. 1999). The two worst 4-year droughts in the instrumental record occurred from 1957 to 1960 and 1980–1983 and were also the worst 4-year periods of tree growth/inferred precipitation during the instrumental period from 1939 to 1990 (Fig. 9).

The full reconstruction is plotted from 1786 to 2016 (Fig. 10) and estimates interesting moisture variability over the eastern equatorial Amazon for the past 230 years. The reconstruction is dominated by interannual and sub-decadal variability, not unlike the instrumental precipitation totals for the eastern Amazon study area (Fig. 9). But the reconstruction also provides preliminary evidence for a decade-long regime of dryness in the mid-nineteenth century (Fig. 10). The worst single year in the entire reconstruction was for 1865, which occurred during seven straight years of reconstructed dryness (1864–1970), part of an 18-year period (1864–1881) of prolonged dryness when only 2 years were above average. This apparent drought regime predates the continuous instrumental measurements of precipitation and streamflow in Amazonia, but earlier discontinuous hydroclimate measurements and documentary information

Fig. 10 The tree-ring estimated February–November precipitation totals are plotted from 1786 to 2016 along with 0.05 and 0.95 semi-parametric prediction intervals. Note the 7-year episode of below mean estimates in the 1980s, six of which were below average in the instrumental data (Fig. 9). A more prolonged dry interval is estimated to have persisted over the Rio Paru sector in the mid-nineteenth Century



might be found from the mid-nineteenth century to provide some historical validation of this reconstructed dry interval (e.g., monthly precipitation totals for Manaus are available from 1870 to 1874 in CRU TS4.00).

Two extended wet episodes are also indicated in the new reconstruction. The mid-twentieth century wet period extended in the reconstruction from 1942 to 1956 and was interrupted by only two dry years (Figs. 9, 10). Rainfall was also above average during this interval in the four-station regional average (Fig. 9). A second regime of elevated rainfall was estimated for the late nineteenth century (1882–1903; Fig. 10) and historical information would again be valuable for testing the validity of this pluvial.

When the observed and proxy rainfall data (February–November) for the eastern Amazon are regressed on gridded sea surface temperatures (averaged for February–April), similar global scale patterns associated with the El Niño/Southern Oscillation (ENSO) are identified in both time series during the 1939–1990 common period (Fig. 11). A 9-point binomial filter was used to remove decadal and longer variability from both the instrumental and reconstructed time series prior to regression with the SST data. The SST patterns associated with the reconstruction are weaker than those observed for the instrumental rainfall data, but both time series are related with cold conditions in the eastern equatorial Pacific and with a gradient of SST anomalies in the South Atlantic (Fig. 11). A very similar pattern of SST association is observed when the regression is based on instrumental precipitation data averaged only for February–April during the heart of the wet season (1939–1990).

The similarity of SST signals in the observed and reconstructed rainfall data provides further support for the proxy climate value of the *Cedrela* chronology from the Rio Paru. The Pacific SST signal in the reconstruction does weaken during the 1991–2016 period, and the signal in the tropical

North Atlantic strengthens (not shown). But a regression of the rainfall reconstruction on the COBE SSTs from 1881 to 2016 is very similar to the global SST patterns illustrated in Fig. 11b.

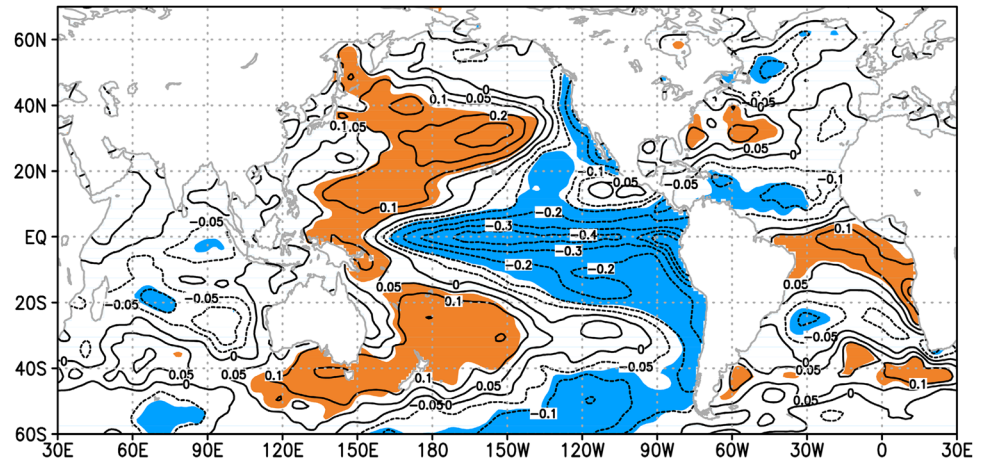
5 Discussion and conclusions

The Rio Paru *Cedrela* collections have provided one of the longest equatorial ($\pm 5^\circ$ N–S) tree-ring chronologies in the world, based on tree-ring data that have been contributed to the NOAA Paleoclimatology Program. These outstanding *Cedrela* trees have well formed concentric growth rings that are obvious and are among the best we have yet found in tropical rainforests. The master dating chronology developed from the Rio Paru has very good chronology statistics reflecting strong internal coherence among the component trees and radii. We are confident that every annual ring on all trees has been exactly dated to the true calendar year of formation. However, this hypothesis can be tested with every new *Cedrela* tree-ring sample dated in the eastern Amazon climate province. Because of the excellent time control provided by the Rio Paru chronology, and the clear definition of the annual growth rings in *Cedrela* from this area, development of additional *Cedrela* chronologies and testing of the hypothesis of exact dating control will now be much easier and perhaps even possible with 12 mm diameter increment cores that can be extracted non-destructively in large numbers from living *Cedrela* in protected forests.

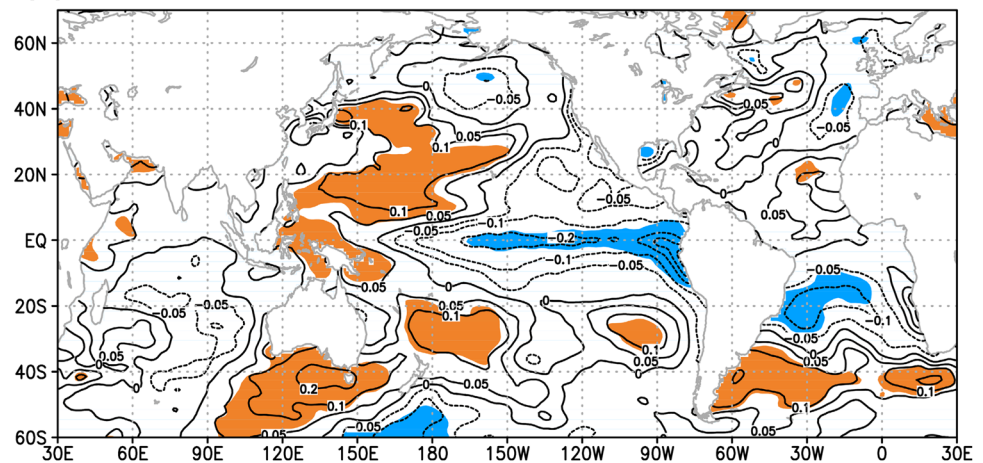
The Rio Paru *Cedrela* chronology is correlated with precipitation, especially February and March rainfall totals at the beginning of the wet season. The ring width correlation with monthly rainfall totals appears to extend to the end of the dry season, which is rarely completely dry in this region. These late dry season correlations improve the overall correlation of Rio Paru tree growth

Fig. 11 The instrumental (a) and the reconstructed February–November precipitation totals (b) for the four-station average from the eastern Amazon were regressed on the gridded COBE SSTs averaged for February–April for the 1939–1990 period. The two precipitation series were first filtered to emphasize interannual to subdecadal variability. Note the similar patterns of SST variability in both the instrumental and reconstructed rainfall series, especially in the cold tongue region of the tropical Pacific. Significant positive and negative relationships are colored orange and blue, respectively ($p < 0.10$). Similar results were obtained using the Kaplan and NOAA gridded SST data sets

(a) Instrumental 4-Station PPT (Feb–Nov), 1939–1990



(b) Reconstructed 4-Station PPT (Feb–Nov), 1939–1990



with precipitation, and if real they may be the combined result of soil moisture recharge, lower evapotranspiration demand, or autocorrelation in monthly precipitation totals.

The changes in the strength, spatial scale, and possibly the seasonality of the tree-ring correlation with rainfall are difficult to explain and may be related to some unknown non-climatic factors affecting tree growth at our moist closed-canopy collection site, the lack of long nearby rainfall recording stations, or to spatial and temporal discontinuities in the instrumental precipitation data. For example, the Porto de Moz and Santarem records included in the CRU TS4.00 data set both end in 1990, and several precipitation stations begin observations in Brazil, French Guiana, and Surinam after 1960 (e.g., Maripasoula, French Guiana). In fact, none of the eight Brazilian stations in the CRU TS4.00 data set that have at least 80 years of observations are located in the eastern Amazon Basin (Manaus is the closest long rainfall station to the Rio Paru site, and they are separated by 800 km).

The apparent changes in the tree growth–climate signal might also arise in part from differences in the regional and large-scale climate influences on tree growth at the Rio Paru. Changes in the two leading modes of precipitation variability, including variability in the position of the Inter-tropical Convergence Zone (ITCZ), may have impacted the reconstructed rainfall record from the Rio Paru. Torralba et al. (2015) demonstrate that the leading mode of rainfall variability in northeast South America (eof1) and the position of the ITCZ are associated with the inter-hemispheric SST gradient in the tropical Atlantic and with tropical Pacific SSTs, but that the combined influence of these SST patterns on the dipole in wet season rainfall totals increased after 1970. An increase in the SST gradient from the tropical to subpolar North Atlantic has also been hypothesized due to SST warming in the tropics and SST cooling in the north due to ice melt, and may have led to a northward shift in the ITCZ resulting in a drier southeastern Amazon (e.g., Malhi et al. 2008; Hilker et al. 2014). The weakening of the climate

signal in the tree-ring data after 1990 might also arise simply from random variability, and the only long term solution will be the development of a well-replicated network of tree-ring chronologies in the eastern Amazon, something that is now much more likely given the high-quality crossdating observed in the new master chronology from the Rio Paru.

In spite of changes in strength and spatial scale, the Rio Paru chronology is significantly correlated with rainfall throughout the instrumental era (1939–2016), and the derived reconstruction is correlated with SSTs in the Pacific and Atlantic similar to the instrumental rainfall data from the eastern Amazon. The preliminary rainfall reconstruction is dominated by notable inter-annual to sub-decadal drought and wet episodes. The reconstruction indicates a decadal dry spell in the mid-nineteenth century and long wet episodes in the late 19th and mid-twentieth century, in spite of the detrending applied to the relatively short forest interior tree-ring time series. The reconstructed mid-nineteenth century drought appears to be as persistent and prolonged as any recorded over the eastern equatorial Amazon during the instrumental era. The implications of this apparent mid-nineteenth century drought are important because it occurred prior to major anthropogenic climate forcing at the regional and global scale, and droughts of the last 20 years are known to have severely impacted forest productivity in Amazonia, resulting in the transient release of carbon dioxide to the atmosphere (Hilker et al. 2014). The true magnitude and persistence of the mid-nineteenth century drought and other decadal precipitation regimes inferred from the *Cedrela* chronology need to be tested with additional historical and proxy data. The Rio Paru chronology and the recently developed *Centropodium* chronologies from the southern Amazon Basin (López et al. 2017) both demonstrate that ring-width chronologies from selected native tree species can be used to reconstruct inter-annual and decadal variability of rainfall and provide a valuable perspective on the limited instrumental observations in Amazonia.

Acknowledgements This study has been funded by the U.S. National Science Foundation (Grant Number AGS-1501321) and is based on the collaboration between the Federal University at Lavras, the Brazilian National Institute of Amazonian Research (INPA) at Manaus, the Argentine Institute of Snow Research, Glaciology, and Environmental Sciences (IANIGLA) in Mendoza, and the University of Arkansas, Fayetteville. D. Granato-Souza was funded in Brazil by the Coordination for the Improvement of Higher Education Personnel (CAPES). We gratefully acknowledge the extensive logistical support and wood donations from Norte Energia (Gilberto Veronese, Miguel Lanzauolo de Paula, Daniel Angelo, Elmar Araújo, José Maria, especially, Jailton Rodriguez Bajos), LEME Energia, the Hudson logging company, and Sr. Evandro Dalmaso and Sra. Eliane Dalmaso of the CEMAL logging firm for their generous logistical support and hospitality. GPCP Precipitation data provided by the NOAA/OAR/ESRL PSD, Boulder, Colorado, USA, from their Web site at <http://www.esrl.noaa.gov/psd/>. COBE SST data provided by the NOAA/OAR/ESRL PSD, Boulder, Colorado, USA, from their Web site at <http://www.esrl.noaa.gov/psd/>.

The indices of the Atlantic Meridional Mode were provided by NOAA at <https://www.esrl.noaa.gov/psd/data/timeseries/monthly/AMM/>. We thank two reviewers for suggestions that helped improve this article. We also acknowledge the data provided by the Climatic Research Unit, University of East Anglia, and the use of the KNMI *Climate Explorer*. The data developed for this article have been contributed to the International Tree-Ring Data Bank at the NOAA Paleoclimatology Program, including all tree-ring data, the instrumental four-station precipitation data, and the derived reconstruction: <https://www.ncdc.noaa.gov/data-access/paleoclimatology-data>.

Funding This study was funded by U.S. National Science Foundation (Grant number AGS-1501321) to the University of Arkansas, and by the Conselho Nacional de Desenvolvimento Científico e Tecnológico (CNPq) to the Federal University of Lavras.

Compliance with ethical standards

Conflict of interest The authors declare that they have no conflict of interest.

References

- Baker JCA, Hunt SFP, Clerici SJ et al (2015) Oxygen isotopes in tree rings show good coherence between species and sites in Bolivia. *Glob Planet Change* 133:298–308
- Becker A, Meyer-Christoffer A, Rudolf B, Schamm K, Schneider U, Ziese M (2013) A description of the global land-surface precipitation data products of the Global Precipitation Climatology Centre with sample applications including centennial (trend) analysis from 1901–present. *Earth Syst Sci Data* 5:71–99. <https://doi.org/10.5194/essd-5-71-2013>
- Bräuning A, Volland-Voigt F, Burchardt I et al (2009) Climatic control of radial growth of *Cedrela montana* in a humid mountain rainforest in southern Ecuador. *Erdkunde* 63:337–345
- Brienen R, Zuidema P (2005) Relating tree growth to rainfall in Bolivian rain forests: a test for six species using tree ring analysis. *Oecologia* 146:1–12. <https://doi.org/10.1007/s00442-005-0160-y>
- Brienen RJW, Helle G, Pons TL, Guyot J-L, Gloor M (2012) Oxygen isotopes in tree rings are a good proxy for Amazonian precipitation and ENSO variability. *Proc Nat Acad Sci* 109:16957–16962. <https://doi.org/10.1073/pnas.1205977109/-DCSupplemental>
- Callede J, Guyot JL, Ronchail J, L'Hote Y, de Oliveira HNE (2004) Evolution du debit de l'Amazone a Obidos de 1903 a 1999/Evolution of the River Amazon's discharge at Obidos from 1903 to 1999. *Hydrol Sci J* 49:85–97
- Cardoso D et al (2017) Amazon plant diversity revealed by a taxonomically verified species list. *Proc Nat Acad Sci*. <https://doi.org/10.1073/pnas.1706756114>
- Chagnon FJF, Bras RL (2005) Contemporary climate change in the Amazon. *Geophys Res Lett* 32:L13703. <https://doi.org/10.1029/2005GL022722>
- Cook ER (1985) A Time series analysis approach to tree-ring standardization. Dissertation, The University of Arizona
- Cook ER, Krusic PJ (2005) Program ARSTAN: a tree-ring standardization program based on detrending and autoregressive time series modeling, with interactive graphics. Manuscript on file, Tree-Ring Lab. Lamont Doherty Earth Observatory of Columbia University, Palisades
- Cook ER, Pederson N (2011) Uncertainty, emergence, and statistics in dendrochronology. *Dendroclimatology, developments in Paleoenvironmental Research*. In: Hughes MK, Swetnam TW, Diaz HF (eds) *Progress and prospects*, vol 11. Springer, Berlin, pp 77–112

- Cook ER, Meko DM, Stahle DW, Cleaveland MK (1999) Drought reconstructions for the continental United States. *J Clim* 12:1145–1162
- Cook ER, Seager R, Heim Jr RR, Vose RS, Herweijer C, Woodhouse C (2010) Megadroughts in North America: placing IPCC projections of hydroclimatic change in a long-term palaeoclimate context. *J Quat Sci* 25:48–61. <https://doi.org/10.1002/jqs.1303>
- Cook ER, Palmer JG, Ahmed M, Woodhouse CA, Fenwick P, Zafar MU, Wahab M, Khan N (2013) Five centuries of upper Indus River flow from tree rings. *J Hydrol* 486:365–375
- Costa MH, Botta A, Cardille J (2003) Effects of large-scale change in land cover on the discharge of the Tocantins River. *Amazonia J Hydrol* 283:206–217
- Crutzen P (1987) Role of the tropics in atmospheric chemistry. In: Dickinson RE (ed) *The geophysiology of Amazonia: vegetation and climate interactions*. Wiley, New York, pp 107–132
- Douglass AE (1941) Crossdating in dendrochronology. *J For* 39:825–831
- Dünisch O, Bauch J, Gasparotto L (2002) Formation of increment zones and intraannual growth dynamics in the xylem of *Swietenia macrophylla*, *Carapa guianensis*, and *Cedrela odorata* (Meliaceae). *IAWA J* 23:101–119
- Fritts HC (1966) Growth rings of trees: their correlation with climate. *Science* 154:973–979
- Gentry AH, Lopez-Parodi J (1980) Deforestation and increased flooding of the Upper Amazon. *Science* 210:1354–1356
- Gloor M, Brienen RJW, Galbraith D, Feldpausch TR, Schöngart J, Guyot JL, Espinoza JC, Lloyd J, Phillips OL (2013) Intensification of the Amazon hydrological cycle over the last two decades. *Geophys Res Lett* 40:1729–1733. <https://doi.org/10.1002/grl.50377>
- Gloor M, Barichivich J, Ziv G, Brienen R, Schöngart J, Peylin P, Barcante Ladvoat Cintra B, Feldpausch T, Phillips O, Baker J (2015) Recent Amazon climate as background for possible ongoing and future changes of Amazon humid forests. *Glob Biogeochem Cycles*. <https://doi.org/10.1002/2014GB005080>
- Griffin RD, Woodhouse CA, Meko DM, Stahle DW, Faulstich HL, Carrillo C, Touchan R, Castro CL, and Leavitt SW (2013) North American monsoon precipitation reconstructed from tree rings. *Geophys Res Lett*. <https://doi.org/10.1002/grl.50184>
- Harris I, Jones PD, Osborn TJ, Lister DH (2014) Updated high resolution grids of monthly climatic observations—the CRU TS3.10 dataset. *Int J Climatol* 34:623–642. <https://doi.org/10.1002/joc.3711>
- Hilker T, Lyapustin AI, Tucker CJ, Hall FG, Myneni RB, Wang Y, Bi J, Mendes de Moura Y, Sellers PJ (2014) Vegetation dynamics and rainfall sensitivity of the Amazon. *Proc Nat Acad Sci* 111:16041–16046. <https://doi.org/10.1073/pnas.1404870111>
- Holmes RL (1983) Computer-assisted quality control in tree-ring dating and measurement. *Tree Ring Bull* 44:69–78
- Intergovernmental Panel on Climate Change (2013) *Climate change 2013: the physical science basis*. In: Stocker TF et al (eds) *Contribution of working group I to the fifth assessment report of the intergovernmental panel on climate change (IPCC)*. Cambridge University Press, Cambridge
- Ishii M, Shouji A, Sugimoto S, Matsumoto T (2005) Objective analyses of sea-surface temperature and marine meteorological variables for the 20th century using ICOADS and the Kobe collection. *Int J Climatol* 25:865–879. <https://doi.org/10.1002/joc.1169>
- Kalnay E et al (1996) The NCEP/NCAR 40-year reanalysis project. *BAMS* 77:437–471
- Khanna J, Medvigy D, Fueglistaler S, Walko R (2017) Regional dry-season climate changes due to three decades of Amazonian deforestation. *Nat Clim Change* 7:200–204
- Lewis SL, Brando PM, Phillips OL, Van der Heijden GMF, Nepstad D (2011) The 2010 Amazon drought. *Science* 331:554. <https://doi.org/10.1126/science.1200807>
- Lopez L, Villalba R (2011) Climate influences on the radial growth of *Centrolobium microchaete*, a valuable timber species from tropical dry forests in Bolivia. *Biotropica* 43:41–49. <https://doi.org/10.1111/j.1744-7429.2010.00653.x>
- Lopez L, Villalba R (2016) Reliable estimates of radial growth for eight tropical species based on wood anatomical patterns. *J Trop For Sci* 28:139–152
- López L, Stahle D, Villalba R, Torbenson M, Feng S, Cook E (2017) Tree-ring reconstructed rainfall over the southern Amazon Basin. *Geophys Res Lett* 44:7410–7418. <https://doi.org/10.1002/2017GL073363>
- Malhi Y, Roberts JT, Betts RA (2008) Climate change and the fate of the Amazon. *Philos Trans R Soc B Biol Sci* 363:1727–1932. <https://doi.org/10.1126/science.1146961>
- Marengo JA, Espinoza JC (2016) Extreme seasonal droughts and floods in Amazonia: causes, trends and impacts. *Int J Climatol* 36:1033–1050. <https://doi.org/10.1002/joc.4420>
- Meko DM, Cook ER, Stahle DW, Stockton CW, Hughes MK (1993) Spatial patterns of tree-growth anomalies in the United States and southeastern Canada. *J Clim* 6:1773–1786
- Nobre CA, Sampaio G, Borma LS, Castilla-Rubio JC, Silva JS, M Cardoso M (2016) Land-use and climate change risks in the Amazon and the need of a novel sustainable development paradigm. *Proc Nat Acad Sci* 113:10759–10768
- Olive DJ (2007) Prediction intervals for regression models. *Comput Stat Data Anal* 51:3115–3122. <https://doi.org/10.1016/j.csda.2006.02.006>
- Paredes-Villanueva K, López L, Cerrillo RMN (2016) Regional chronologies of *Cedrela fissilis* and *Cedrela angustifolia* in three forest types and their relation to climate. *Trees*. <https://doi.org/10.1007/s00468-016-1391-8>
- Richey JE, Nobre C, Deser C (1989) Amazon River discharge and climate variability: 1903–1985. *Science* 246:101–103
- Schneider U, Finger P, Meyer-Christoffer A, Rustemeier E, Ziese M, Becker A (2017) Evaluating the hydrological cycle over land using the newly-corrected precipitation climatology from the Global Precipitation Climatology Centre (GPCC). *Atmosphere* 8:52. <https://doi.org/10.3390/atmos8030052>
- Schöngart J, Bräuning A, Barbosa ACMC., Lisi CS, de Oliveira JM (2017) Dendroecological studies in the neotropics: history, status and future challenges. In: Amoroso M, Daniels L, Baker P, Camarero J (eds) *Dendroecology, ecological studies (analysis and synthesis)*, vol 231. Springer, Cham, pp 35–73
- Schulman E (1956) *Dendroclimatic changes in semi-arid America*. University of Arizona Press, Tucson
- Seber A, Lee J (2003) *Linear regression analysis*. Wiley, Hoboken
- Stokes MA, Smiley TL (1996) *An introduction to tree-ring dating*. University of Arizona Press, Tucson
- ter Steege H, Pitman NCA, Sabatier D, Baraloto C, Salomão RP et al (2013) Hypredominance in the Amazonian tree flora. *Science* 342:325–334
- ter Steege H, Vaessen RW, Cardenas-Lopez D, Sabatier D, Antonelli A, Mota de Oliveira S, Pitman NCA, Jorgensem PM, Salomao RP (2016) The discovery of the Amazonian tree flora with an updated checklist of all known tree taxa. *Sci Rep* 6:29549. <https://doi.org/10.1038/srep29549>
- Torralba V, Rodríguez-Fonseca B, Mohino E, Losada T (2015) The non-stationary influence of the Atlantic and Pacific Niños on North Eastern South American rainfall. *Front Earth Sci* 3. <https://doi.org/10.3389/feart.2015.00055>
- van der Schrier G, Barichivich J, Briffa KR, Jones PD (2013) A scP-DSI-based global data set of dry and wet spells for 1901–2009. *J Geophys Res Atmos* 118:4025–4048
- Villalba R, Cook ER, Jacoby GC, D'Arrigo RD, Veblen TT, Jones PD (1998) Tree-ring based reconstructions of northern Patagonia precipitation since AD 1600. *Holocene* 8:659–674

- Villalba R, Lara A, Masiokas MH, Urrutia R, Luckman BH, Marshall GJ (2012) Nat Geosci 5:793. <https://doi.org/10.1038/NGEO1613>
- Vinod HD (2006) Maximum entropy ensembles for time series inference in economics. *J Asian Econ* 17:955–978. <https://doi.org/10.1016/j.asieco.2006.09.001>
- Wagner FH et al (2014) Climate seasonality limits leaf carbon assimilation and wood productivity in tropical forests. *Biogeosciences* 13:2537–2562
- Wang H, Fu R (2007) The influence of Amazon rainfall on the Atlantic ITCZ through convectively coupled Kelvin waves. *J Clim* 20:1188–1201
- Wigley TML, Briffa KR, Jones PD (1984) On the average value of correlated time series, with applications in dendroclimatology and hydrometeorology. *J Clim Appl Meteorol* 23:201–213